Computers and Concrete, Vol. 6, No. 6 (2009) 473-490
DOI: http://dx.doi.org/10.12989/cac.2009.6.6.473

Load carrying capacity of deteriorated reinforced concrete columns

Mucip Tapan†

Department of Civil Engineering, Yuzuncu Yil University, Zeve Kampusu, Van 65080, Turkey

Riyad S. Aboutaha‡

Department of Civil & Environmental Engineering, Syracuse University, 255 Link Hall, Syracuse, NY 13244, USA

(Received September 15, 2008, Accepted September 16, 2009)

Abstract. This paper presents a new methodology to evaluate the load carrying capacity of deteriorated non-slender concrete bridge pier columns by construction of the full P-M interaction diagrams. The proposed method incorporates the actual material properties of deteriorated columns, and accounts for amount of corrosion and exposed corroded bar length, concrete loss, loss of concrete confinement and strength due to stirrup deterioration, bond failure, and type of stresses in the corroded reinforcement. The developed structural model and the damaged material models are integrated in a spreadsheet for evaluating the load carrying capacity for different deterioration stages and/or corrosion amounts. Available experimental and analytical data for the effects of corrosion on short columns subject to axial loads combined with moments (eccentricity induced) are used to verify the accuracy of proposed model. It was observed that, for the limited available experimental data, the proposed model is conservative and is capable of predicting the load carrying capacity of deteriorated reinforced concrete columns with reasonable accuracy. The proposed analytical method will improve the understanding of effects of deterioration on structural members, and allow engineers to qualitatively assess load carrying capacity of deteriorated reinforced concrete bridge pier columns.

Keywords: corrosion; deterioration model; concrete columns; bridge evaluation; P-M interaction diagrams.

1. Introduction

Many existing concrete structures deteriorate or exhibit extensive damage due to lack of attention to durability issues e.g., the effects of corrosion and freezing and thawing cycles. Evaluation of such structures is required to determine strength and safety at the time of investigation, and to determine the degree of damage that can be tolerated before shoring or repair is required. Today, USA civil infrastructure requires major rehabilitation. For the last 30 years, bridges in excess of 6.1 meters in total length located on public roads have received periodic inspections to ensure safety to the public. According to the FHWA report "Status of the Nation's Highways, Bridges, and Transit: 2004

† Ph.D., E-mail: mtapan@yyu.edu.tr
‡ Associate Professor, Corresponding author, E-mail: rsabouta@syr.edu

Conditions and Performance”, overall, there are 162,869 bridges that are deficient within the USA highway bridge network. This represents 27.5 percent of the total inventory of highway bridges when bridges are weighted equally (FHWA 2004). According to the FHWA report, corrosion damage caused by deicing salts is considered as one of the main problems that cause a bridge structure to be structurally deficient.

Current knowledge of the load carrying capacity of deteriorated or damaged reinforced concrete columns is limited. After damage or deterioration has taken place, the primary concern is to know the remaining load carrying capacity of the existing concrete member. This is particularly important for highway bridges where deterioration due to durability issues is a concern. Currently, inspectors assess the bridge members in a visual fashion based on engineering expertise and experience, and in some cases supplemented by non-destructive tests. These assessment procedures form the basis for assessing the structural condition of a bridge. Rating for the bridge system is taken as the minimum of the component ratings that are subjectively assessed by inspectors using condition rating scales.

Better understanding of the effects of deterioration on the structural performance of deteriorated reinforced concrete columns, will enhance the currently used inspection procedures (i.e. condition rating) to plan strategic and cost-effective rehabilitation methods. This paper presents a methodology for estimation of actual load carrying capacity of deteriorated reinforced concrete columns. The method is based on development of interaction diagrams using the damaged geometry and material properties of deteriorated concrete and reinforcement. The procedure could easily be adapted in AASHTO manuals for evaluation of deteriorated columns, and other structural evaluation guides/ manuals. For ease of use, the developed method has been implemented in a spreadsheet for ease of application.

2. Properties of deteriorated materials

The behavior and strength of reinforced concrete members is controlled by the size and shape of the members, the stress-strain properties of the concrete, and the reinforcement. Material behavior of deteriorated concrete and reinforcement is investigated, and stress-strain properties of the deteriorated concrete and reinforcement is used in proposed model. The material behavior discussed in this section is used for determining load carrying capacity of deteriorated reinforced concrete members.

2.1. Concrete

The calculation of the flexural strength of reinforced concrete sections is usually based on an assumed ultimate concrete compression strain of 0.003 and a compression stress block evaluated from the concrete stress-strain curve up to that strain. However, concrete that is restrained in the directions at right angles to the applied stress has the ability to carry significant stresses at high strains.

A concrete column’s section is generally confined by transverse reinforcement in the form of closely spaced steel spirals or hoops. At low axial concrete stress levels, the transverse reinforcement is hardly stressed and thus the concrete is unconfined. The confinement becomes more effective at stresses approaching the uniaxial concrete strength, f_c', where the transverse strains become very high because of the progressive internal cracking and the concrete bears out

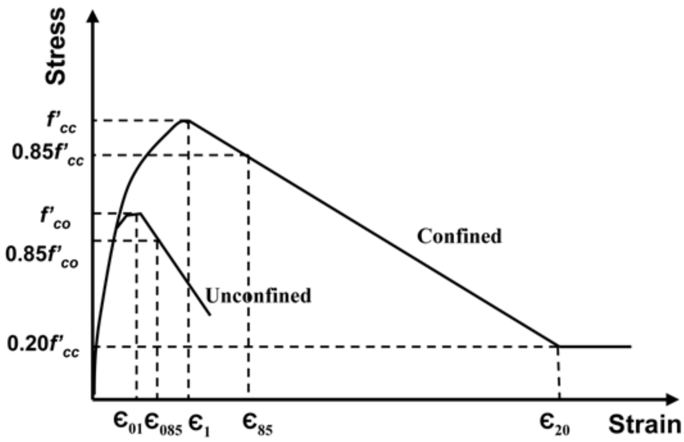

Fig. 1 Confined concrete model used in the proposed model (After Saatcioglu and Ravzi 1992)

against the transverse reinforcement, which then applies a confining reaction on the concrete, which becomes confined. Tests by many investigators have shown that such confinement can considerably improve the stress-strain characteristics of concrete once it starts to expand laterally.

The confined concrete model developed by Saatcioglu and Razvi (1992) is used in the proposed model. The model is based on the computation of confinement pressures starting from the material and geometric properties of columns. Different distributions of pressure, resulting from different arrangements of equivalent uniform pressures are expressed in terms of equivalent pressures. The equivalent uniform pressure f_{le} is derived from the average pressure f_l. The average pressure is calculated from tensile forces in transverse reinforcement, with due consideration given to the steel area and yield strength. Fig. 1 shows the confined concrete model used in the proposed model.

2.1.1. Effect of stirrups corrosion on concrete strength

Stirrup corrosion have significant effects on load carrying capacity of the reinforced concrete columns (i.e. relatively larger cross-section reduction, loss of concrete confinement because of loss of bond and loss of anchorage).

These significant effects are expected because stirrups start corroding earlier than the longitudinal reinforcement and since they are smaller in diameter, same corrosion rate leads to larger relative reductions in stirrup cross-sections. When the stirrup starts to corrode the confinement effect of stirrups is reduced because of the loss of bond between reinforcement and concrete. When the cover to the longitudinal reinforcement cracks, the load carrying capacity starts to decrease at a faster rate due to the reduction of stirrup anchorage. This results in longer unsupported longitudinal reinforcement lengths, which leads to premature buckling of longitudinal reinforcement, and consequently decrease in the load carrying capacity of the column.

Stirrups in a reinforced concrete column are used to provide shear resistance, confine the concrete core, and brace the longitudinal reinforcement. They are, however, more vulnerable to corrosion than longitudinal bars due to both a lesser cover and a greater surface/cross-sectional area ratio. They start corroding earlier than the longitudinal reinforcement and since the same attack penetration leads to larger section reductions, corrosion of stirrups has significant effect both on axial and moment carrying capacity and shear capacity of deteriorated reinforced concrete columns. Thus, in the proposed model this effect is taken into consideration by using concrete confinement model

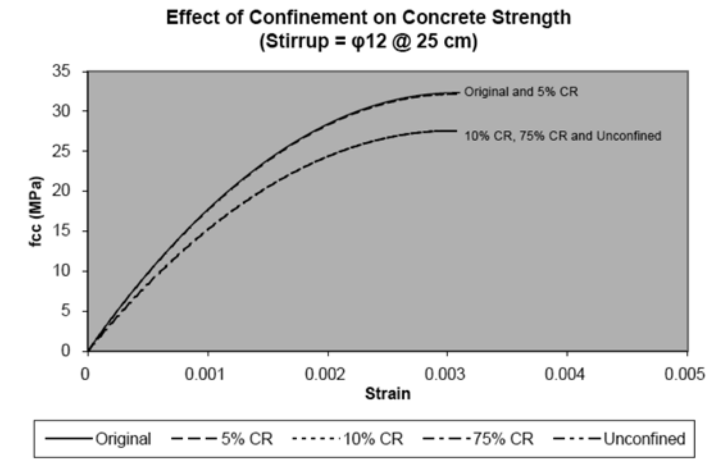

Fig. 2 Effect of corrosion on concrete strength for a concrete column having 27.6 MPa original cube strength (transverse reinforcement is φ12 spaced at 25 cm)

developed by Saatcioglu and Razvi (1992). It is assumed that there is no bond (i.e. no confinement effect of stirrups) between stirrups and concrete after cover cracking. Since corrosion of stirrups affect the bond with surrounding concrete, the model developed by Saatcioglu and Razvi (1992) is used to include the effect of corrosion on concrete strength. Fig. 2 shows an example on how the confined concrete model is affected by corrosion of stirrups. Effect of stirrups' corrosion on concrete confinement is investigated for different deterioration stages and/or corrosion amounts in another study (Tapan 2007).

2.2. Steel reinforcement

Reinforcements subjected to corrosion attack suffer loss of strength and loss of ductility, thus models developed for undeteriorated reinforcement cannot be used for predicting the nonlinear behavior of corroded steel reinforcement. The AASHTO manual provision concerning the procedure for the safety assessment of a deteriorated structure indicates that analysis using mathematical modeling should include the damaged geometry and material properties. Therefore, the geometry and material properties of corroded reinforcement is used to successfully develop the stress-strain relationship of corroded reinforcement under compression and tension separately.

2.2.1. Steel reinforcement under tension

The residual capacity of corroded reinforcing bars was investigated by Du *et al.* (2005). The mechanism of the reduction of capacity of corroded reinforcement was investigated by performing both accelerated and simulated corrosion tests on bare bars and on bars embedded in concrete (the test conditions were more onerous than those that should be present under actual field conditions). The author's results agreed reasonably well with those obtained under natural corrosion conditions. Therefore the results can be applied in practice with good confidence.

The influence of type and diameter of reinforcement on its residual capacity was discussed by Du *et al.* (2005). The experimental results showed that, due to local attack penetration, the residual cross-section of a corroded bar is no longer round and also varies considerably along its circumference and its length. Although the force-extension curves of corroded bars were similar to those of non-corroded bars for up to 16% corrosion, their residual yield and ultimate forces decreased more rapidly than their average cross-sectional area, and therefore, their residual strength decreased significantly. A simple equation by Du *et al.* (2005) was adopted to predict the residual capacity of corroded reinforcing bars.

$$f = (1 - 0.005 \cdot Q_{corr}) \cdot f_y \tag{1}$$

Where; f and f_y are yield strengths of corroded and non-corroded reinforcement, respectively.

Average cross-sectional area of corroded reinforcement, A_s, and the amount of corrosion, Q_{corr} (%), were estimated as;

$$A_s = A_{so} \cdot (1 - 0.01 \cdot Q_{corr}) \tag{2}$$

$$Q_{corr} = 0.046 \cdot \frac{I_{corr}}{d} \cdot t \tag{3}$$

Where; A_{so} is the initial cross-sectional area of non-corroded reinforcement, and Q_{corr} is the amount of corrosion of reinforcement, d is the diameter of non-corroded reinforcement, I_{corr} is the corrosion rate of reinforcement in real structure ($\mu A/cm^2$), and t is the time elapsed since the initiation of corrosion (years).

In another study by Du *et al.* (2005) on the effect of corrosion on ductility of reinforcing bars, it was reported that, corrosion of reinforcement does not change significantly the strength ratio, hardening strain and elastic modulus of corroded reinforcement, because corrosion removes iron ions only from the bar surface and does not change the nature and composition of the remaining steel reinforcement. Since corrosion does not change substantially the shape of the stress-strain curve of reinforcement, it was assumed that corroded reinforcement has a similar curve to that of non-corroded reinforcements and has a definite yield plateau, as shown in Fig. 3 (Du *et al.* 2005).

The empirical equations, proposed by Du *et al.* (2005) to assess the residual strength and ductility of corroded reinforcement embedded in concrete is used to calculate the yield and ultimate strain of the corroded reinforcement.

The predicted nonlinear characteristic for corroded bars is simplified as a bilinear stress-strain relationship in this study and is given in Fig. 4.

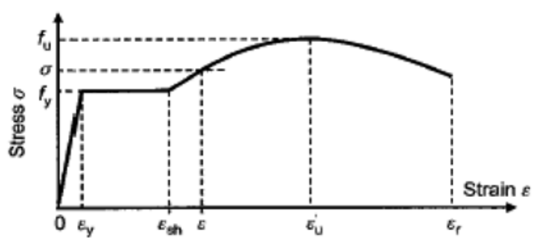

Fig. 3 Stress-strain curve of corroded reinforcement (Du *et al.* 2005)

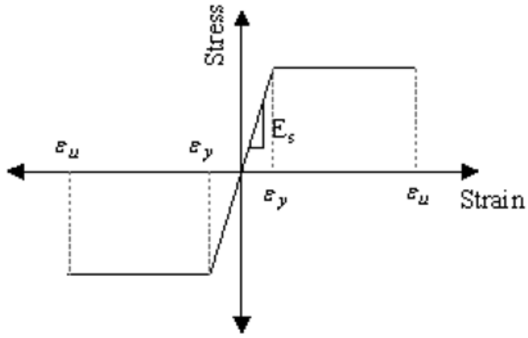

Fig. 4 Idealized stress-strain curve for corroded reinforcement

Although these tests on mechanical behavior of corroded reinforcement have been confined to bars in tension, it is reasonable to assume that strength in compression may be similarly impacted, however, since once the cover of the structural member spalls off because of corrosion, the compressed bars are likely to buckle. This effect is taken into account and details are given in next section.

$$\varepsilon_u = (1.0 - 0.05 \cdot Q_{cor}) \cdot \varepsilon_{uo} \tag{4}$$

$$\varepsilon_y = (1.0 - 0.05 \cdot Q_{cor}) \cdot \varepsilon_{yo} \tag{5}$$

Where; ε_u, is the ultimate strain of corroded reinforcement, Q_{corr} is the corrosion rate, ε_{uo}, is the ultimate strain of original reinforcement, ε_y, is the yield strain of corroded reinforcement, and ε_{yo}, is the yield strain of original reinforcement.

2.2.2. Steel reinforcement under compression - buckling of deteriorated reinforcement in compression

Axial load carrying capacity of a column decreases with reduction in cross-sectional area of reinforcement, and loss of bond. If the unbonded length of a corroded reinforcement exceeds a critical length under compression, it may buckle before yielding. Several researchers (Mau and El-Mabsout 1989, Monti and Nuti 1992, Bayrak and Sheikh 2001) reported that the inelastic buckling behavior of a reinforcing bar is very sensitive to unsupported bar length-to-bar diameter ratio. It was observed that the load-carrying capacity and ductility decreased as the L/d ratio increased.

For a deteriorated column, once the cover spalls off, compressed reinforcements are likely to buckle. In other words, if the exposed corroded bar length, exceeds a critical length; the reinforcement will buckle before reaching its yield capacity and load carrying capacity of the deteriorated column will be reduced (i.e. calculations using yield strength will no longer be correct). This condition was taken into consideration, as described in this section, for P-M interaction calculations.

The likelihood of reinforcement buckling in concrete members has been established in most related studies by analyzing the unsupported length of reinforcement with the linearized (small deformations) version of the Euler buckling theory for slender members.

The critical axial stress in the reinforcing bar associated with this buckling condition is estimated from;

$$f_{cr} = \frac{\pi^2 \cdot E \cdot I_b}{L^2 \cdot A_b} \tag{6}$$

Where, E is the modulus of elasticity of the rebar; L is the unsupported length of the bar, which varies with the assumed end conditions; I is the moment of inertia and A_b is the area of the bar.

In previous studies, differences had been observed between theoretical and experimental values of column deformation at buckling (Pantazopoulou 1998). One of the reasons for the differences is that, the Euler model ignores the composite action between concrete and reinforcement. However, because deterioration reduces the bond strength between concrete and reinforcement, Euler buckling model is conceptually acceptable to evaluate the effect of the reinforcement buckling on axial load carrying capacity.

On the other hand, the design strength for flexural buckling compression members subjected to axial compression through the centroidal axis is given by following equations in LRFD Manual;

$$P_n = A_g \cdot f_{cr} \tag{7}$$

$$f_{cr} = (0.658^{\lambda_c^2}) \cdot f_y \quad \text{for } \lambda_c \leq 1.5 \tag{8}$$

$$f_{cr} = \left(\frac{0.877}{\lambda_c^2}\right) f_y \quad \text{for } \lambda_c > 1.5 \tag{9}$$

where;

$$\lambda_c = \frac{K \cdot L}{r \cdot \pi} \cdot \sqrt{\frac{f_y}{E}}$$

A_g= Gross area of member, in^2
f_y = Specified minimum yield stress (f in Eq. 12 is used instead of f_y for the corroded reinforcement, ksi)
E = Modulus of elasticity, ksi
K = Effective Length factor
L = Laterally unbraced length of member, in
r = Governing radius of gyration about the axis of buckling, in

In this study, a methodology using LRFD buckling stress is developed to account for the effect of the length of exposed rebars on the critical buckling force and further used for developing the interaction diagrams for deteriorated reinforced concrete columns. Stress-strain diagram for exposed bars are developed, as shown in Fig. 5, for Grade 60 (f_y = 420 MPa) bars. In addition, the change in magnitude of critical buckling force, for different L_{exp}/d_{cor} ratios, is also investigated as shown in Fig. 6. In these calculations, exposed bars are assumed to be pinned at both ends and mechanical properties of corroded reinforcement are used to calculate critical buckling stress.

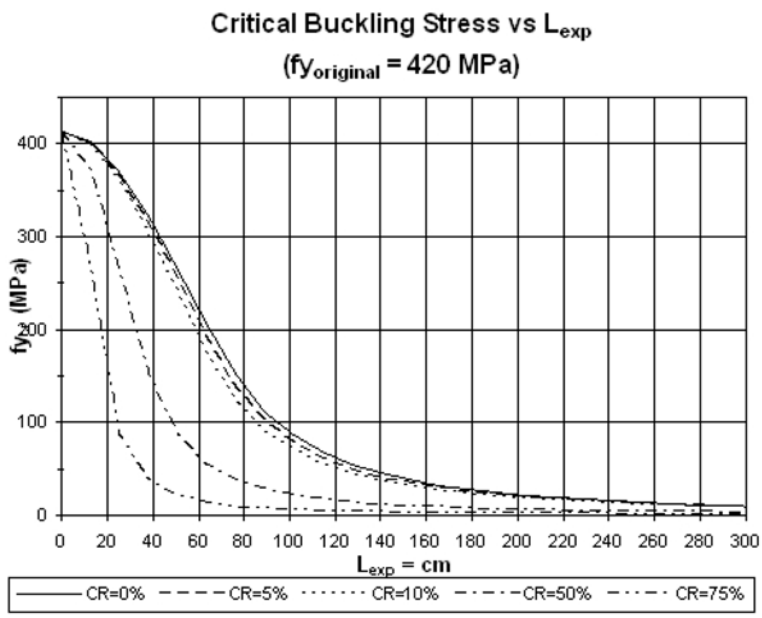

Fig. 5 Effect of amount of corrosion and exposed bar length on critical buckling stress of reinforcement

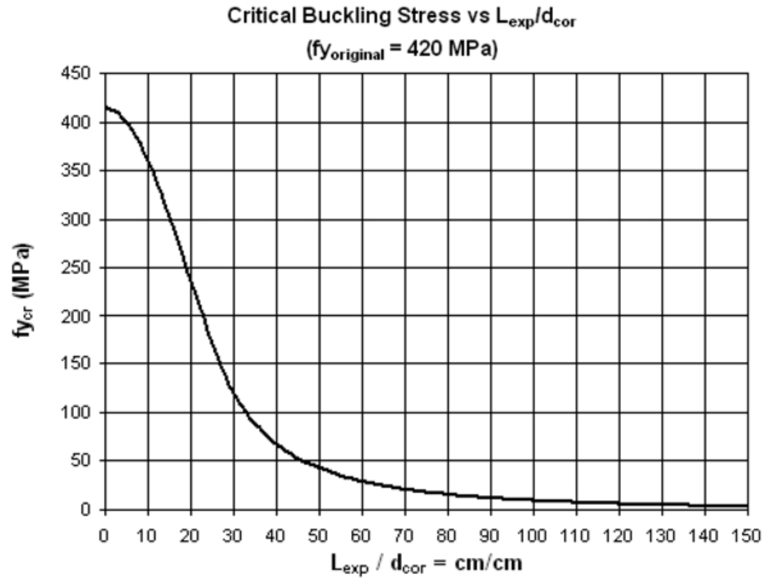

Fig. 6 Effect of exposed bar length/corroded diameter on critical buckling stress of reinforcement

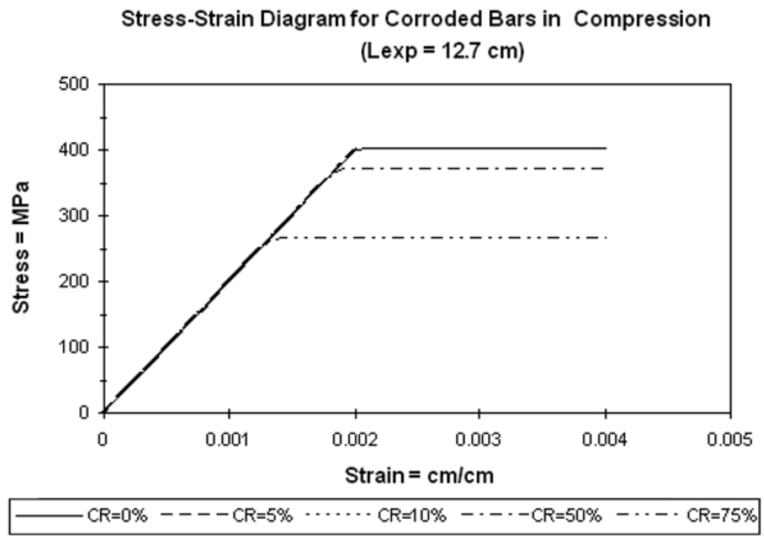

Fig. 7 Stress - Strain relation for corroded reinforcement under compression ($F_{y\ original}$ = 420 MPa, *Lexp* = 12.7 cm)

Fig. 5 shows the relation between the critical buckling stresses and exposed (unsupported, corroded) bar lengths for different corrosion amounts. Fig. 6 demonstrates the relation between L_{exp}/d_{cor} ratio and critical buckling stress. Observing Figs. 5 and 6, it can be stated that there is dramatic decrease in critical buckling stress as exposed bar length over corroded reinforcement diameter ratio increases.

Using this methodology the stress-strain diagram for corroded bars under compression is idealized for different corrosion amounts and exposed bar lengths, as illustrated in Figs. 7 through 9. This idealized stress-strain relationship is used in the proposed model for reinforcement under compression.

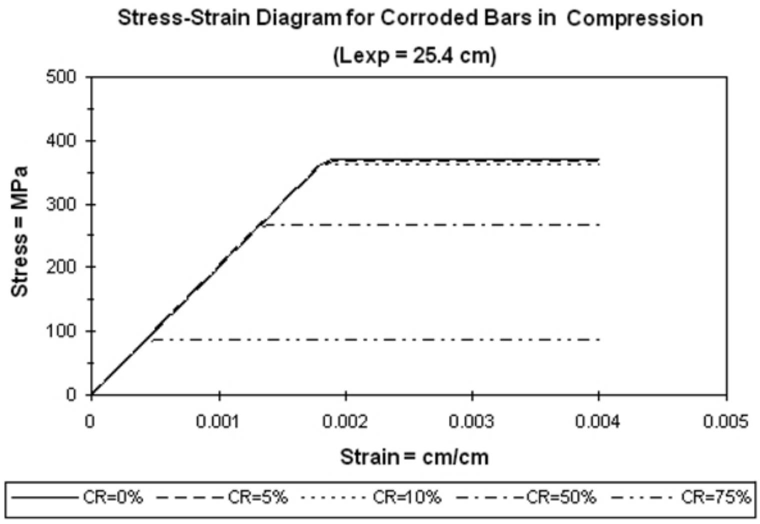

Fig. 8 Stress - Strain relation for corroded reinforcement under compression ($F_{y\ original}$ = 420 MPa, *Lexp* = 25.4 cm)

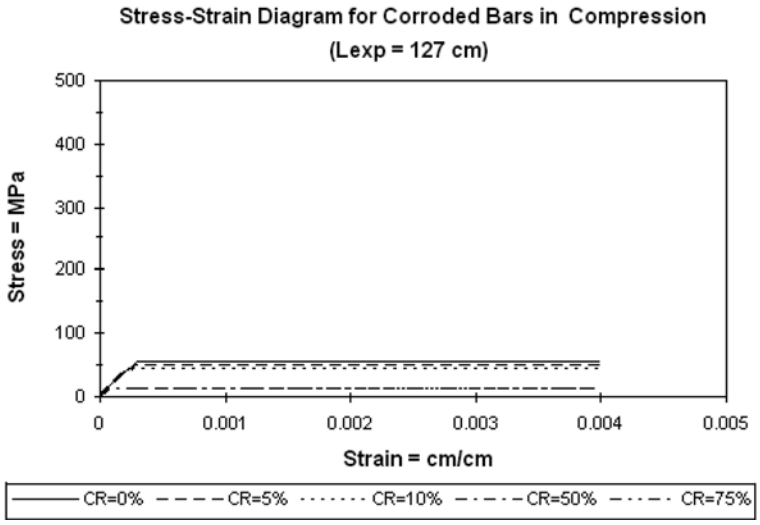

Fig. 9 Stress - Strain relation for corroded reinforcement under compression ($F_{y\ original}$= 420 MPa, *Lexp* = 127 cm)

3. Interaction diagram for concrete columns

Although it is possible to derive a family of equations to evaluate the load carrying capacity of columns subjected to combined bending and axial loads, these equations are tedious to use (MacGregor 1997). For this reason, interaction diagrams for columns are generally computed by assuming a series of strain distributions, each corresponding to a particular point on the interaction diagram, and computing the corresponding values of *P* and *M*. When enough of such points have been computed, the results are summarized in an interaction diagram. For conventional reinforced concrete members, strains and stress changes can be determined in any typical section along the span using equilibrium equations, stress-strain relations, and strain compatibility. Such an analysis assumes that perfect bond exists between reinforcement and concrete, and implies that the strain change under load in the reinforcement is equal to the strain change in the concrete at the level of reinforcement. However, non-uniform reinforcement corrosion along the height and cross-section of the member leads to deterioration of bond. Therefore, conventional strain compatibility does not apply as-is in computing stresses in corroded reinforcement (i.e. the strain changes along the corroded reinforcement length (The average strain in the concrete over the unbounded length of the corroded bar is used as the strain in the unbounded corroded steel bar)), and conventional method based on strain compatibility cannot be used without some modifications to determine actual capacity of deteriorated reinforced concrete members.

The following assumptions are made for computing the interaction diagrams of deteriorated reinforced concrete columns:

- Boundary conditions for exposed bars are assumed to be pinned-pinned, and the exposed bar length of all corroded bars are assumed to be equal.
- The modified material properties of corroded reinforcement under compression is assumed to be same as those of corroded bar under tension. However, for corroded bars in compression, if the exposed corroded bar length exceeds a critical length; the reinforcement will buckle before reaching its yield capacity. In such cases, buckling stress is used for load carrying capacity calculation of the deteriorated column.
- It is assumed that, corrosion of reinforcement does not change significantly the general shape of the stress-strain diagram of reinforcement. Therefore it is assumed that corroded reinforcement has a similar curve to that of non-corroded reinforcements and has a well-definite yield plateau.
- Beyond the cover cracking corrosion level, complete bond deterioration is assumed between concrete and reinforcement.
- As the corrosion of the steel stirrups reduces the steel section of the stirrups, and causes bond deterioration between the stirrups and the concrete, it is assumed that corroded stirrups would not produce any confining effect on the concrete core, and consequently, in this case the unconfined material properties of concrete are used for the concrete core.
- Strain in corroded (unbonded) reinforcement is assumed to be equal to average strain change in adjacent concrete over the exposed reinforcement length (Eq. 21).
- Although the experimental results and visual inspections showed that due to local attack penetration, the residual cross-section of a corroded bar is no longer round and varies considerably along its circumference and its length, reduction in reinforcement due to corrosion is assumed to be uniform. It is also assumed that corrosion is uniform along the height of the exposed length of the corroded rebar.
- Corroded stirrups provide insignificant bracing to longitudinal bars, therefore, the stiffness of the stirrups along the height of the exposed bar length is assumed to be small enough to be ignored in calculations.
- Uniaxial compressive strength of cover concrete after cracking is neglected in the strength calculations.

Almusallam *et al.* (1996) investigated the effect of reinforcement corrosion on the bond strength between steel and concrete. Their study showed that when reinforcement corrosion was in the range of 4 to 6%, bond failure had occurred suddenly. At this level of reinforcement corrosion, a large slip was noted as the ultimate failure of the bond occurred due to the splitting of the specimens. Inspections results of some common case studies of existing concrete bridge columns deteriorated by corrosion of reinforcing steel bars in concrete supported the above finding (Aboutaha 2004). It was also observed that, as the corrosion level increases, corrosion pressure has limited effect on softening of concrete through the concrete core. After formation of a longitudinal crack along the height of a corroded reinforcing bar, the bar deflects by corrosion pressure towards the weakest part and concrete cover spalls off.

Modeling of regions of unbonded reinforcement is based on the average change in the adjacent concrete over the exposed reinforcement length. At the critical section, the stress in an unbonded reinforcement will increase more slowly than that in bonded reinforcement. This is because any strain in an unbonded reinforcement will be distributed throughout its entire length. The average strain in concrete over the exposed length (L) is given by

$$\varepsilon_{c,ave} = \varepsilon_s = \frac{\Delta L}{L} = \int_0^L \frac{\Delta \varepsilon_c}{L} dx \tag{21}$$

The interaction diagram calculation process is illustrated in Fig. 10 for one particular deterioration case and strain distribution. The cross-section is illustrated in Fig. 10(a) and one assumed strain distribution is shown in Fig. 10(b). The maximum compressive strain is set at 0.003, corresponding to failure of the section. The location of the neutral axis and the strain in each level of reinforcement are computed from the strain distribution. This information is then used to compute the size of the compression stress block and the stress in each layer of reinforcement, as shown in Fig. 10(c). The forces in the concrete and the steel layers, are computed by multiplying the stresses by the areas on which they act. Finally, the axial force P_n is computed by summing the individual forces in the concrete and steel, and the moment M_n is computed by summing the moments of these forces about the plastic centroid of the section. These values of P_n an M_n represent one point on the interaction diagram.

A flowchart is developed, to explain the various steps used to evaluate load carrying capacity of deteriorated reinforced concrete columns by developing P-M interaction diagrams, as shown in Fig. 11.

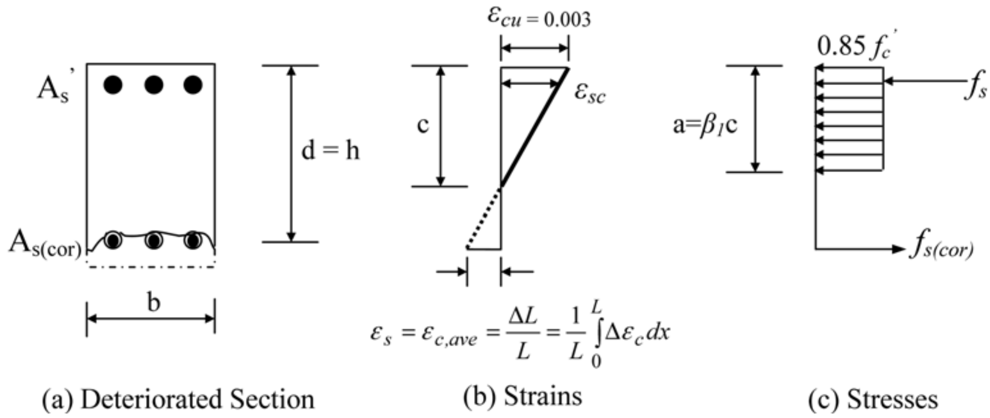

Fig. 10 Calculations of stress and strains for a given section and strain distribution

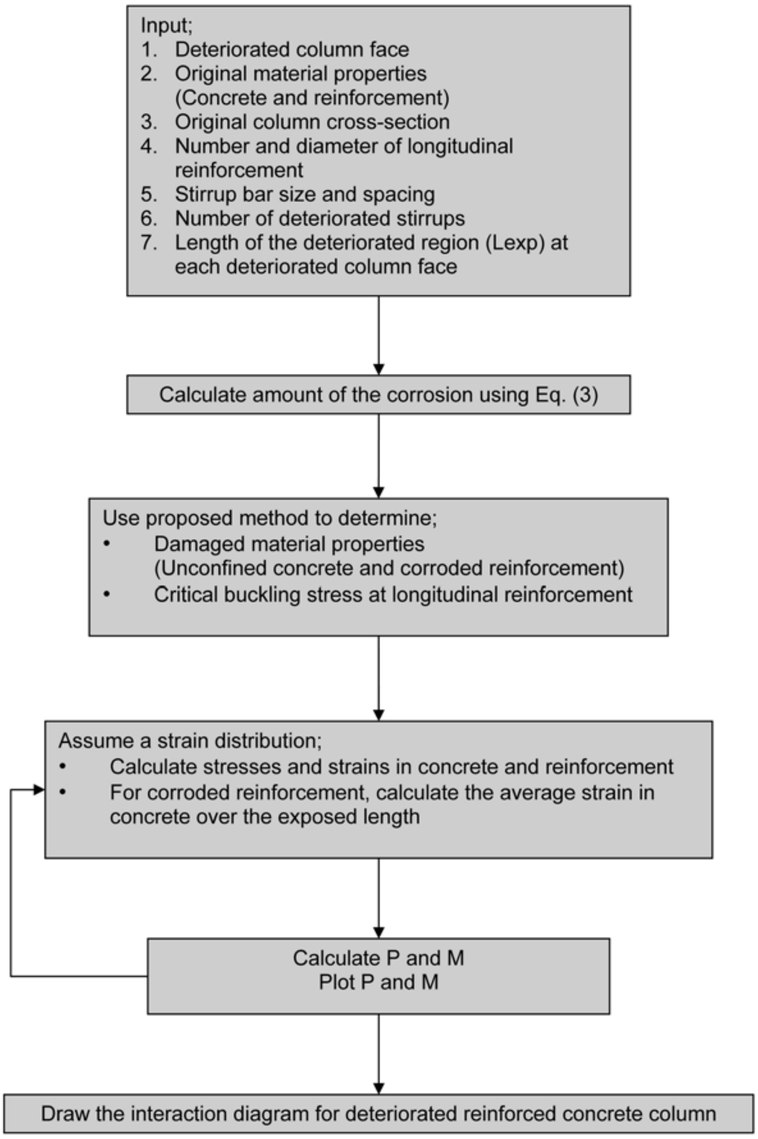

Fig. 11 Flow chart for developing P-M interaction diagrams for deteriorated reinforced concrete columns

3.1. Model verification

Rodriguez *et al.* (1997) conducted an experimental study using 24 columns to establish the relationship between the level of corrosion and the structural performance of deteriorated concrete columns. Three types of column with 200 mm by 200 mm cross section and 2000 mm length with end stiffening were tested. Type 1 columns had four 8 mm ribbed bars as the main reinforcement with 6 mm ribbed stirrups at 100 mm spacing. Type 2 columns had four 16 mm main bars with 6 mm stirrups at 150 mm spacing. Type 3 columns had eight 12 mm main bars with 6 mm stirrups at 150 mm spacing. Figs. 13 and 14 show all three types of columns that were tested as well as the loading

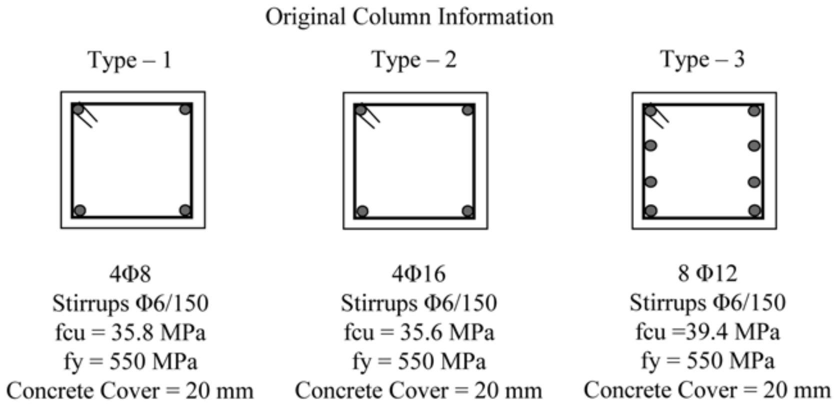

Fig. 12 Cross-sections of the columns tested by Rodriguez *et al.* (1997)

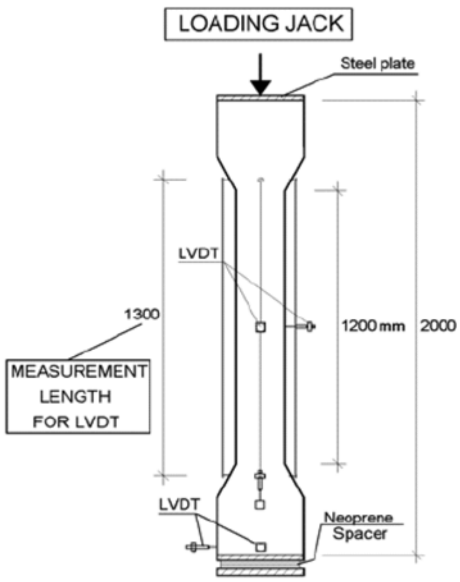

Fig. 13 Loading test arrangement and elevation of the tested columns (Rodriguez *et al.* 1997)

test arrangements.

In order to induce corrosion, 3% sodium chloride (by weight of cement) was added to the mixing water, and a current of 100 μA/cm^2 was applied to all of the reinforcement in the 1200 mm central test section for approximately 100-200 days to obtain the required level of corrosion.

Although these columns are axially loaded, nominal moments are present due to a combination of the non-uniformity of the corrosion, imperfections in the casting and testing regime and, at later stages, spalling. Test data are only available for the effects of accelerated corrosion on short columns subject to an axial load combined with eccentricity-induced moments.

Rodriguez *et al.* (1997) found three main aspects seem to affect the behavior of the corroded columns: the deterioration (spalling) of the concrete section, the increase of the load eccentricity due to asymmetric deterioration of the concrete cover and the likely reduction of reinforcement

Table 1 Summary of experimental results in the loading tests for Type -2 Columns

COLUMN TYPE	COLUMN No.	DELAMINATION LOAD (*)		ULTIMATE LOAD				
		AXIAL FORCE (kN)	MEAN STRAIN (–)	AXIAL FORCE (kN)	MEAN STRAIN (–)	No. OF BROKEN STIRRUPS	ECCENTRICITY (+)	
							e_x	e_y
2	21 (Control)			1680	2.7		8.2	2.3
	22 (Control)			1702	2.6		2.1	5.4
	23	993	1.1	1080	2.2	1-2	22.2	15.6
	24	999	1.2	1040	2	1	20.5	14.1
	25	934	1	1091	1.8	3	13.8	16.4
	26	890	1.1	1135	2.1	3-4	1.4	7.4
	27	847	1	973	1.8	4	3.2	4.6
	28	975	1.4	997	1.8	4	1.9	5.5

(*) Load value when initiation of delamitation of concrete cover was observed.
(–) Mean strain at the midspan zone, in %o, on the four sides of the column
(+) Eccentricity of the load, in mm, obtained from the strain values on each side of the column.

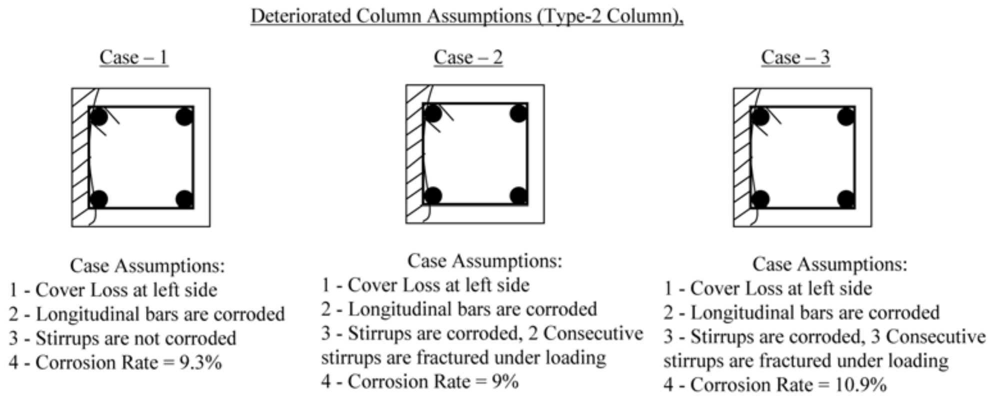

Fig. 14 Deteriorated Type - 2 columns represented by interaction diagrams developed by Rodriguez *et al.* (1997)

strength due to premature buckling. They developed interaction diagrams for two types of tested columns.

The first one, for Type-1 columns, was developed using conventional models considering the reduced bar section, either the complete or the reduced concrete section (assuming no concrete cover at the four sides). Two eccentricity values of 0 mm and 20 mm were assumed for interaction diagram calculations.

The second one, for Type-2 columns, was developed using actual deteriorated concrete section with several unsupported exposed bar lengths. Therefore interaction diagrams developed for Type-2 columns are used for verification of proposed model. According to supplied experimental test results, the representing experimental tests are also plotted on the same graph for comparison purposes. Since, only two out of six experiments are represented by analytically developed interaction diagrams, these two experiments are used for verification (i.e. column 23 and column 25). Summary of

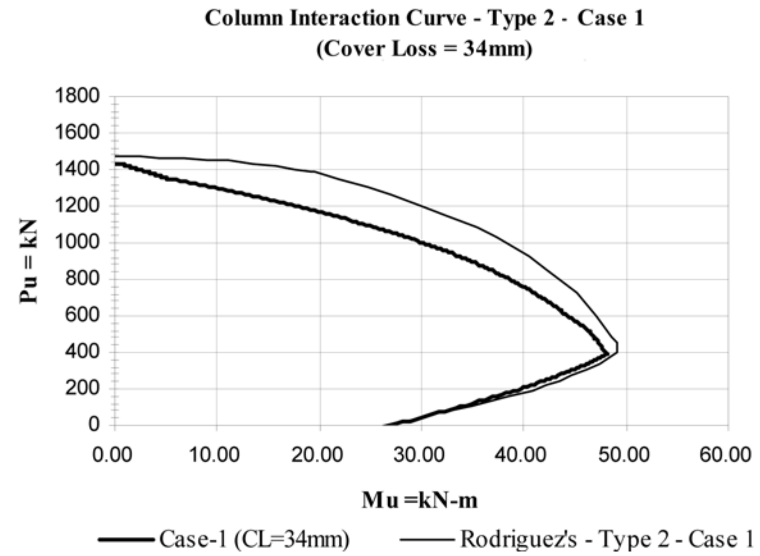

Fig. 15 Comparison of the column interaction diagrams for Type - 2, Case - 1 column

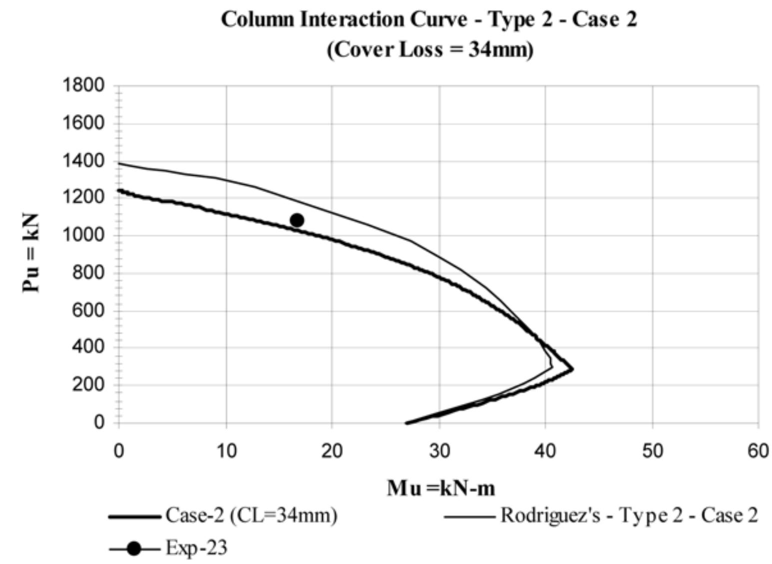

Fig. 16 Comparison of the column interaction diagrams for Type - 2, Case - 2 column

the Type-2 columns experimental results are tabulated in Table 1 below. For simplicity, the experiments represented by interaction diagrams were assigned a case name. Those cases are illustrated in Fig. 15 below with brief information about the deterioration level.

Fig. 16 shows both the interaction diagram developed by Rodriguez *et al.* (1997) and the one developed by proposed model for Case - I, where it was assumed that the left side of the concrete cover was deteriorated. For this case Rodriguez *et al*. (1997) did not take into account the buckling of compression bars. Since experimental results show that in all six deteriorated columns there are broken stirrups, this case cannot be represented by any of the experiments and therefore Fig. 16

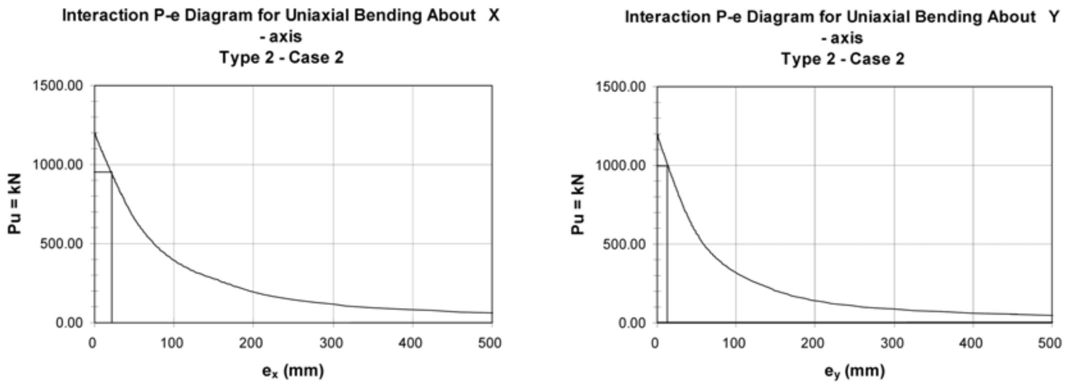

Fig. 17 Interaction P-e diagram for uniaxial bending about *x* and y axis for Column 23

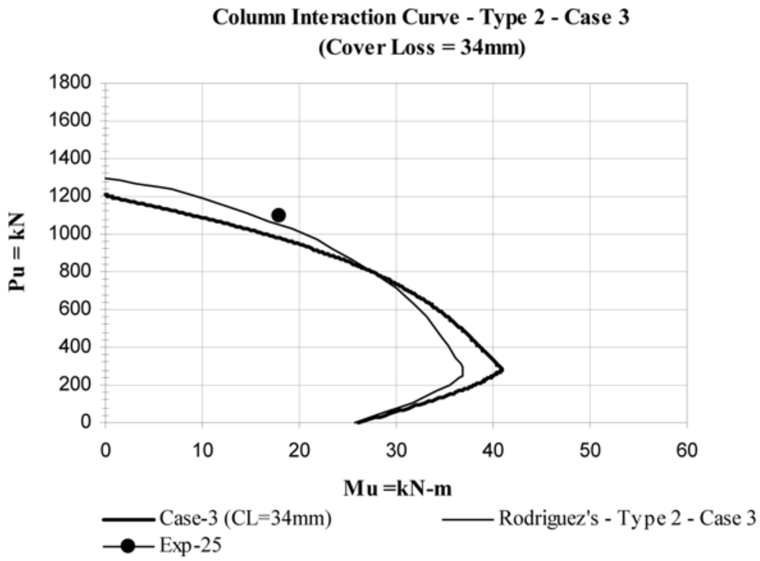

Fig. 18 Comparison of the column interaction diagrams for Type - 2, Case - 3

does not show the experimental result for comparison purposes.

Figs. 16 and 18 show the interaction diagrams developed for Column 23 and Column 25 using proposed model, and the interaction diagram that was developed by Rodriguez *et al.* (1997). For comparison purposes the results of the experimental tests are also plotted on same diagrams.

The interaction diagrams developed using the proposed model reasonably agree with the ones developed by Rodriguez *et al.* (1997). However, in compression field the developed model shows lower strength. That is probably because of different models used for computing buckling stresses, residual strength of corroded reinforcement and strains at corroded regions. In both cases the results of the experiments are not in the failure region determined by proposed model. The result of column 23 and column 25 is just above the interaction diagram developed by using proposed model. Although, there is only one set of data available that contains minimum sufficient data to be used for verification of the proposed model, the comparison of experimental results and interaction diagrams yields that the proposed model seems to accurately represent the behavior of corroded

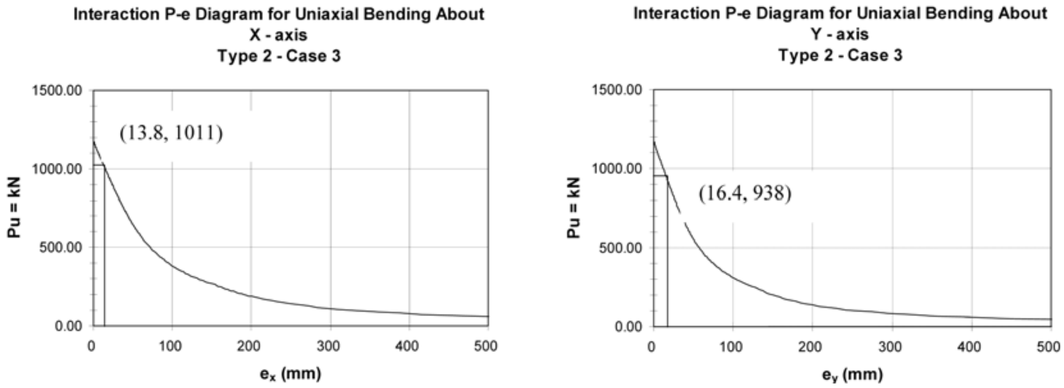

Fig. 19 Interaction P-e diagram for uniaxial bending about *x* and *y* axis for Column 25

reinforced concrete columns. And for the limited available experimental data the proposed model is considered conservative. However, further comparisons should be done with the availability of new experimental data.

Analysis of the results using Bresler Reciprocal Load Method for Column 23:

$$\frac{1}{P_n} \approx \frac{1}{P_i} = \frac{1}{P_x} + \frac{1}{P_y} - \frac{1}{Po}$$

$$\frac{1}{Pi} = \frac{1}{933} + \frac{1}{970} - \frac{1}{1207.6}$$

$$P_n = 784.53kN \le P_u = 1080kN$$

Analysis of the results using Bresler Reciprocal Load Method for Column 25:

$$\frac{1}{P_n} \approx \frac{1}{P_i} = \frac{1}{P_x} + \frac{1}{P_y} - \frac{1}{Po}$$

$$\frac{1}{Pi} = \frac{1}{1011} + \frac{1}{938} - \frac{1}{1182.3}$$

$$P_n = 826.85kN \le P_u = 1091kN$$

4. Conclusions

This paper presents a method for evaluating load carrying capacity of deteriorated reinforced concrete columns that can be adopted into currently used condition evaluation method by construction of the full P-M interaction diagrams. This method may be used for calculating nominal member resistance (structural capacity) of the deteriorated structural member as inspected.

The damaged geometry and material properties are incorporated in the proposed method. Material behavior of deteriorated concrete and reinforcement steel is investigated and stress-strain properties of the deteriorated concrete and reinforcement steel are developed, and used in the proposed model.

The method accounts for the effects of various corrosion variables such as reduction in reinforcement strength under tension and compression, loss of bond, corroded bar length, loss of concrete cover, and cross-sectional asymmetry. In addition, the model accounts for the loss of concrete strength because of stirrup deterioration (i.e. loss of confinement). The developed structural model and the damaged material models are integrated in a spreadsheet for evaluating the load carrying capacity for different deterioration stages and/or corrosion amounts.

Available experimental and analytical data for the effects of corrosion on short columns subject to axial loads combined with moments (eccentricity induced) were used to verify the accuracy of proposed model. The results show that the proposed model is conservative (for the limited available experimental data) and is capable of predicting the load carrying capacity of deteriorated reinforced concrete columns with reasonable accuracy.

The proposed analytical method will improve the understanding of effects of deterioration on the structural performance of concrete columns, and allow engineers to assess the condition and the load carrying capacity of reinforced concrete bridge pier columns with greater accuracy. Due to the fact that each bridge substructure needs to be individually evaluated, the developed spreadsheet will allow inspectors and engineers to assess a number of deterioration scenarios quickly. Ultimately, using proposed approach will help reduce repair costs and avoid over-conservative ratings that would result in a more uniform level of safety of concrete bridges in the United States.

References

Aboutaha, R.S. (2004), *Guide for Maintenance, and Rehabilitation of Concrete Bridge Components with FRP Composites-Research into Practice*, TIRC & NYSDOT, NY, USA.

Almusallam, A.A., Al-Gathani, A.S., Aziz, A.R. and Rasheeduzzafar (1996), "Effect of Reinforcement Corrosion on Bond Strength", *Constr. Build. Mater.*, **10**(2), 123-129.

American Association of State Highway and Transportation Officials (2003), *Guide manual for condition evaluation and load and resistance factor rating (LRFR) of highway bridges,* 1st Edition, AASHTO Publications. Washington DC, USA.

Bayrak, O. and Sheikh, S.A. (2001), "Plastic hinge analysis", *J. Struct. Eng-ASCE*, **127**(9), 1092-1100.

Du, Y.G., Clark, L.A. and Chan, A.H.C. (2005), "Effect of corrosion on ductility of reinforcing bars", *Mag. Concrete Res.,* **57**(7), 407-419.

Du, Y.G., Clark, L.A. and Chan, A.H.C. (2005), "Residual capacity of corroded reinforcing bars", *Mag. Concrete Res.,* **57**(3), 135-147.

Federal Highway Administration (2004), *Status of the Nation's highways, bridges, and transit: 2004 Conditions and performance report to congress*, http://www.fhwa.dot.gov/policy/2004cpr/index.htm (Aug. 13, 2006).

MacGregor, J.G. (1997), *Reinforced Concrete Mechanics and Design*, 3rd Edition, Prentice Hall, New Jersey.

Mau, S.T. and El-Mabsout, M. (1989), "Inelastic buckling of reinforcing bars", *J. Eng. Mech.*, **115**(1), 1-17.

Monti, G., and Nuti, C. (1992), "Nonlinear cyclic behavior of reinforcing bars including buckling", *J. Struct. Eng-ASCE*, **118**(12), 3268-3284.

Pantazopoulou, S.J. (1998), "Detailing for reinforcement stability in RC members", *J. Struct. Eng-ASCE*, **124**(6), 623-632.

Saatcioglu, M. and Razvi, S. (1992), "Strength and Ductility of Confined Concrete", *J. Struct. Eng-ASCE*, **118**(6), 1590-1607.

Tapan, M. (2007), *Strength Evaluation of Deteriorated Reinforced Concrete Bridge Columns,* PhD. Dissertation, Syracuse University, USA.

CM